PHYSICAL REVIEW C VOLUME 44, NUMBER 4 OCTOBER 1991

Small-angle two-neutron and two-proton correlations in 30A MeV heavy-ion reactions

B. Jakobsson, B. Norén, A. Oskarsson, and M. Westenius
Department of Physics, University of Lund, Sölvegatan 14, S-223 62 Lund, Sweden

M. Cronqvist, S. Mattson, M. Rydehell, and Ö. Skeppstedt
Department of Physics, Chalmers University of Technology, S-412 96 Göteborg, Sweden

J. C. Gondrand, B. Khelfaoui, S. Kox, F. Merchez, C. Perrin, and D. Rebreyend
Institut des Sciénces Nucléaires de Grenoble, Université de Grenoble, 53 avenue des Martyrs, F-380 26 Grenoble CEDEX, France

L. Westerberg
The Svedberg Laboratory, University of Uppsala, Box 533, S-751 21 Uppsala, Sweden

S. Pratt
Department of Physics, University of Wisconsin, Madison, Wisconsin 53706
(Received 16 January 1991)

Two-neutron correlations at small relative momentum in ^{20}Ne+C and ^{20}Ne+Co reactions at 30A MeV exhibit correlation functions dominated by the attractive final-state interaction. The results are consistent with two-proton data. The data suggest large apparent emission sources for both reactions with contributions from both pre-equilibrium emission and evaporation.

Momentum correlations between particles are known to be sensitive to the space-time characteristics of the emission source. Two-photon correlations have been used to determine the size of stellar objects [1]. Two-pion [2] and two-proton [3] correlations have been utilized to extract information about the emission sources in nuclear reactions [4–15].

At high energies, where the early parts of the emission processes could be expected to be very rapid, interaction volumes may be well established. Correlations in nucleus-nucleus collisions at these energies indicate in general the existence of extended sources which depend little on the sizes of the nuclei.

At lower energies the time difference between the emission of two nucleons ($\Delta\tau$) can never be neglected [11–13]. A reliable time scale must be introduced in order to extract useful information about the source size. Systematic determinations of the space-time characteristics with respect to energy, masses, or particle momenta are, however, always useful for the understanding of the reaction dynamics.

It is often stressed that mutual (and mean-field) Coulomb interaction obscures the quantum interference information in case of p-p (p-p and p-n) correlations. Data from n-n correlations are indeed scarce and come so far from high-energy p-nucleus reactions [16] and low-energy nucleus-nucleus reactions very close to the Coulomb barrier [17]. In the former case final-state dominated correlation functions are observed, whereas in the latter case an anticorrelation for zero-momentum difference is reported, indicating pure quantum interference (antisymmetrization effect) due to the very large scattering length.

We report in this paper on the first results of n-n and p-p correlations from 30A MeV nucleus-nucleus collisions. The experimental setup (Fig. 1) consisted of four hexagonal (~15 cm in diameter and 15 cm thick) Bicron BC-501 liquid scintillator neutron detectors [18] combined with the EMRIC, CsI+MWPC (multiwire proportional chamber) interferometer [19] for charged particles. EMRIC contained 16 CsI (area 4×4 cm^2, 10 cm thick) scintillators placed at an angle of 29° with a distance of 66 cm from the target and with a two-plane multiwire proportional chamber in front of it. Neutron detectors were placed 3.5 m from the target behind the holes and above and below EMRIC (Fig. 1). Charged-particle identification in EMRIC as well as neutron/gamma discrimination on the liquid scintillators is made by pulse-shape analysis, i.e., by integration of QDC (charge-

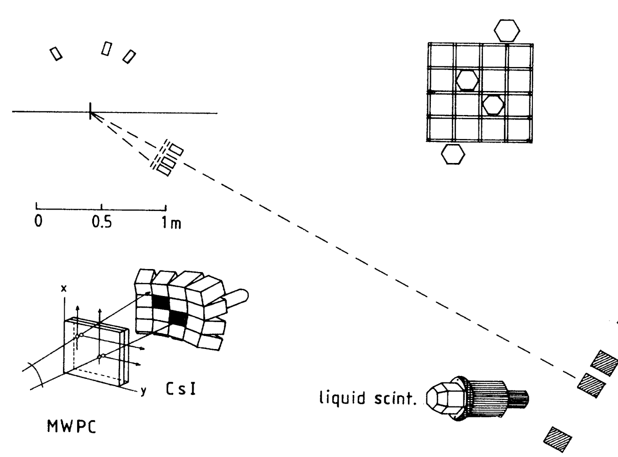

FIG. 1. A schematic picture of the experimental setup. The distance between the neutron detector pairs is 28, ~60, and 115 cm for close, medium distant, and distant pairs.

to-digital converter) pulses during different time gates. The details of EMRIC and the neutron detectors are discussed elsewhere [18,19].

Two-particle triggers were normally recorded. Neutron energies were measured by their time of flight, taken as the time difference between the rf accelerator signal and the neutron detector signal. The total time resolution, determined from the width of the γ peak, is 3 ns including the spread from the beam pulse (~ 1.2 ns) and the scintillators (~ 1 ns). The neutron detection efficiency as a function of the energy was calculated with the Monte Carlo code of Cecil, Anderson, and Madey [20] [Fig. 2(a)].

A 30A MeV ^{20}Ne beam from the SARA coupled cyclotron facility was bombarding ~ 1 mg/cm^2 targets of C and Co. All detectors ($\Delta\theta = 2.5°$) were placed in the angular interval 24°–34°. The energy threshold was 1.5 MeV for neutrons and 8 MeV for protons. For n-n correlations the closest detectors allow for relative momenta of $q = |\mathbf{p}_1 - \mathbf{p}_2|/2 \geq 1.2$ MeV/c and the most distant pairs for $q \geq 9.0$ MeV/c. The hit position of each neutron is homogeneously randomized within the front area, which, in fact, changes the correlation function little as compared to assumed hits in the detector centers alone.

The correlation function $R(q)$ is given by

$$R(q)+1 = C\frac{N_c(q)}{N_{\rm nc}(q)} , \qquad (1)$$

where N_c stands for true coincidences and $N_{\rm nc}$ for noncorrelated events. C is the normalization constant obtained from the assumption that $R(q)=0$ for $q > 50$ MeV/c. $N_{\rm nc}$ is obtained by randomly choosing 100 noncorrelated $\mathbf{p}_1$ particles. $N_{\rm nc}$ is then normalized to the number of two-particle events in N_c. Both N_c and $N_{\rm nc}$ have a q-dependent efficiency correction (for n-n) since, e.g., large q events will predominantly include large $p_{1,2}$ momenta. The general trend in the correction is to decrease the peak height.

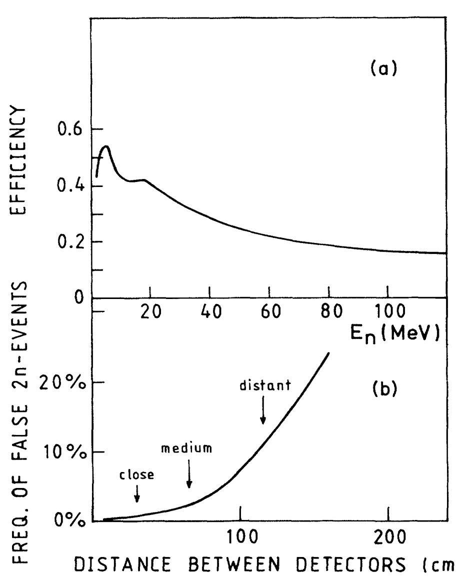

FIG. 2. (a) The energy dependence of the neutron detector efficiency [20]. (b) The frequency of false two-neutron coincidences due to scattering in EMRIC as a function of the distance between the detectors.

Three kinds of background corrections that must be considered are the following.

(i) The amount of random coincidences are estimated from the coincidence time spectra. These show small constant background levels with an amount of such events always $< 1\%$.

(ii) Neutrons scatter elastically or inelastically in EMRIC. Practically all charged particles ($E_p \leq 55$ MeV) are stopped by the 2 mm stainless steel housing of the neutron detectors so we consider only false nn' or $n'n''$ correlations. An analytic determination of this background, utilizing empirical energy-dependent isotropical doubly differential cross sections (mainly elastic n+CsI), gives $1\times10^{-3}N_0$ false correlations for close detectors and $2\times10^{-3}N_0$ for distant pairs. N_0 is the (inclusive) number of neutrons entering one neutron detector. The number of $2n/1n$ events (measured without coincidence requirement) is equal to 0.11, 0.06, and 0.01 for close, medium distant, and distant detector pairs. The frequency of false $2n$ events [Fig. 2(b)], increases with increasing distance between the detectors. It is introduced as a correction to the $R(q)$ function by estimating the q shift (Δq, here estimated from a Monte Carlo simulation) for all the n-n' events which originally fall within the EMRIC area. In fact, Δq approaches zero when q is very large or very small and it peaks ($\Delta q \simeq 140$ MeV/c for distant pairs) for $q = 30$ MeV/c. In Fig. 3 we show that the total effect of this correction is small even for the distant detector combination. The error bars in Figs. 3 and 4 contain statistical errors only but all background corrections, discussed here, have been introduced. At present we cannot explain the low values of R in the $15 \leq q \leq 40$ MeV/c interval for the distant detector pairs but the number of such correlations is very small (1.5% of all).

(iii) Scattering from one neutron detector into another (crosstalk) is the most serious kind of background for a dense array fo neutron detectors [21] where no shielding between detectors is used. Because of the larger and variable distances between the detectors in this experiment the crosstalk is smaller and controllable. A comparison between the measured $R(q)$ function for all events and that representing only events inside the kinematically allowed region for elastic $C(n,n')$ and $H(n,n')$ scattering showed little difference. The energy-dependent crosstalk effects were simulated with a Monte Carlo program that introduces all important (n,n'), $(n,n'p)$, $(n,2n)$, and $(n,n'\gamma)$ scattering channels [21]. An analytic determination of the crosstalk for 10 MeV neutrons, $(3^{+3}_{-2})\times10^{-3}N_0$, $(5^{+3}_{-2})\times10^{-4}N_0$, and $(9\pm4)\times10^{-5}N_0$ for close, medium, and distant pairs, confirms the simulated values of $(4\pm2)\times10^{-3}N_0$, $(6\pm1)\times10^{-4}N_0$, and $(8\pm7)\times10^{-5}N_0$, respectively. From the $2n/1n$ ratios given in (ii) we obtain the amount of false crosstalk events which is noticeable ($\sim 5\%$) only for the close detector combination.

Figure 4 shows the total $R(q)$ for ^{20}Ne+C and ^{20}Ne+Co collisions. The p-p correlations, measured with

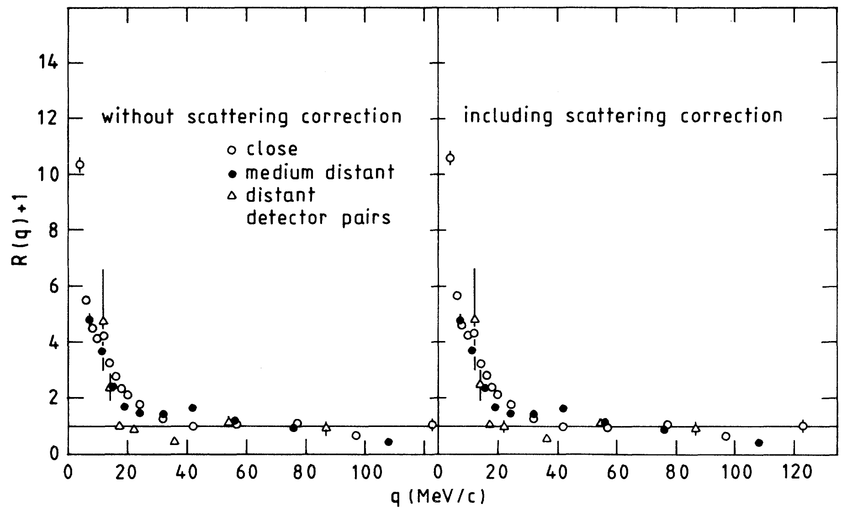

FIG. 3. Correlation functions for close, medium distant, and distant detector pairs in ^{20}Ne+C collisions before and after the introduction of the scattering correction.

the EMRIC modules simultaneously are also shown. As pointed out earlier the points with $q \leq 5$ MeV/c (n-n) could be affected somewhat from the assumption of a homogeneous distribution of hits over the detector area.

The correlation function that is used for comparison with the data is derived from the formula given by Pratt and Tsang [22] and by Gong *et al.* [15].

$$1+R(\mathbf{p},\mathbf{q})=\int d^3r\,F_p(\mathbf{r})|\phi(\mathbf{q},\mathbf{r})|^2\,,$$

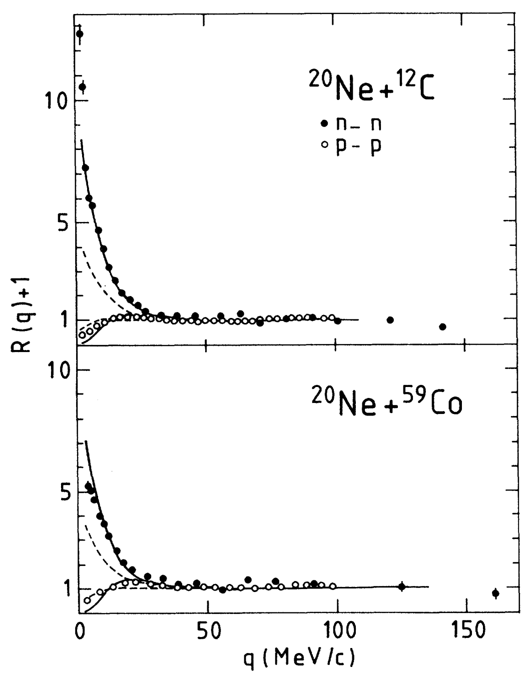

FIG. 4. Correlation functions for p-p and n-n correlations in ^{20}Ne+C reactions (upper) and ^{20}Ne+Co reactions (lower) at 30A MeV. The solid curves come from a $\Delta\tau=0$ interferometry calculation [22] where the source size is set to 5.0 fm. The dashed curves come from a fusion-evaporation calculation.

where $F_p(\mathbf{r})$ is defined by

$$F_p(\mathbf{r})=\frac{\int d^3\,\tfrac{1}{2}\,\mathbf{r}_1+\mathbf{r}_2 f(\mathbf{p},\mathbf{r}_1,t_>)f(\mathbf{p},\mathbf{r}_2,t_>)}{\left|\int d^3\mathbf{r}\,f(\mathbf{p},\mathbf{r},t_>)\right|^2}\,. \quad (2)$$

Here p is the average momentum of the nucleon pair and $t_>$ is the time corresponding to the ceasing of the particle interaction [15]. The relative wave function ϕ is found by solving the Schrödinger equation using the Reid soft core potential. The phase-space distribution, $f(\mathbf{p},\mathbf{r},t)$, can be extracted from any theoretical model that predicts the emission probability. This approach differs from that of Koonin [3] only in the way that integration over time now may be incorporated as in the case of the evaporation calculation below. A detailed discussion about the formulation is given in another paper [15].

Provided that the major part of the nucleons in the two-nucleon correlations comes from very fast processes, a $\Delta\tau=0$ assumption is acceptable. Calculations, where $\mathbf{r}_i$ and $\mathbf{p}_i$ are generated from Gaussian probability distributions, are presented (solid curves) in Fig. 4. The nucleon emission may well be dominated by an evaporation source and such calculations, based on initial complete fusion, are also presented (dashed curves). Since the correlation function depends on the momentum distribution chosen we use the experimental one.

The correlation functions are dominated by the attractive final-state interaction and in addition for p-p correlations the Coulomb interaction. The p-p and n-n correlation curves are consistent with each other, as shown by the $\Delta\tau=0$ calculations, at least for $q>12$ MeV/c. For $q<10$ MeV/c there may be a difference between the p-p and n-n correlation functions, but this region may be disturbed by the difference in the momentum cutoff. All data indicate large apparent source sizes as reported earlier for charged-particle correlations at similar energies [5,7–9]. The calculations shown in Fig. 4 are made for a radius of 5.0 fm and the agreement is somewhat better for the less complicated n-n correlation function. A slight but insignificant tendency of a larger source size for the Ne+Co reaction might be observed. The evaporation calculations have been performed under the assumption that complete fusion takes place initially without any loss of thermal energy due to compression or any loss of nucleons due to nonthermal pre-equilibrium processes. This calculation underestimates the experimentally observed correlation peaks (at $q=0$ for n-n and $q\simeq 20$ MeV/c for p-p correlations), though the Weisskopf evaporation process is treated in a time-dependent way with decreasing temperature.

In conclusion p-p and n-n correlations exhibit consistent correlation functions dominated by final-state effects and the anticorrelation for small q which was found for reactions close to the Coulomb barrier [17] is not observed. Instead, our correlation functions are similar to those reported for p-nucleus collisions at high energies [16]. Provided that the emission process is very fast ($\Delta\tau=0$) large apparent source sizes are found with little dependence on the target size. A pure evaporation source cannot explain the structures of the correlation functions, indicating the expected mixture of nonthermal pre-equilibrium emission and evaporation.

We are grateful for the support from the SARA accelerator staff. P. Désesquelles is thanked for introducing us to the crosstalk simulation program. The financial support from IN2P3 and the Swedish Natural Science Research Council is acknowledged. One of us (B.N.) acknowledges the warm hospitality of ISN, Grenoble.

[1] R. Hanbury-Brown and R. Q. Twiss, Philos. Mag. **45**, 663 (1954).
[2] G. Goldhaber, S. Goldhaber, W. Lee, and A. Pais, Phys. Rev. **120**, 300 (1960).
[3] S. E. Koonin, Phys. Lett. **53**, 544 (1977).
[4] S. Nagamiya, Nucl. Phys. A **400**, 399c (1983).
[5] W. G. Lynch *et al.*, Phys. Rev. Lett. **51**, 1850 (1983).
[6] H-A. Gustafsson *et al.*, Phys. Rev. Lett. **53**, 544 (1984).
[7] L. Carlén *et al.*, Phys. Scr. **34**, 475 (1986).
[8] D. Cebra *et al.*, Phys. Lett. B **227**, 336 (1989).
[9] J. Pochodzalla *et al.*, Phys. Rev. C **35**, 1695 (1987).
[10] P. Dupieux *et al.*, Phys. Lett. B **200**, 17 (1988).
[11] P. A. de Young, M. S. Gordon, Xiu qin Lu, R. L. McGrath, J. M. Alexander, D. M. de Castro Rizzo, and L. C. Vaz, Phys. Rev. C **39**, 128 (1989).
[12] D. Ardouin, P. Lautridon, D. Durand, D. Goujdami, F. Guilbault, C. Lebrun, A. Peghaire, J. Quebert, and F. Saint-Laurent, Nucl. Phys. A **495**, 57c (1989).
[13] J. M. Alexander *et al.*, in *Proceedings of the CORINNE Workshop, Nantes, France, 1990,* edited by D. Ardouin (World Scientific, London, 1990), p. 154.
[14] S. Kox *et al.*, in *Proceedings of the CORINNE Workshop* (Ref. [13]), p. 93.
[15] W. G. Gong, W. Bauer, C. K. Gelbke, and S. Pratt, Phys. Rev. C **43**, 781 (1991).
[16] Yu. D. Bayukov *et al.*, Phys. Lett. B **189**, 291 (1987).
[17] W. Dünnweber, W. Lippig, D. Otten, W. Assman, K. Hartmann, W. Hering, D. Konnerth, and W. Trombik, Phys. Rev. Lett. **65**, 297 (1990).
[18] S. E. Arnell *et al.*, Nucl. Instrum. Methods (submitted).
[19] F. Merchez, S. Kox, C. Perrin, J. Mistretta, J. C. Gonrand, L. N. Imouk, P. Gretillat, and E. Schwartz, Nucl. Instrum. Methods, Phys. Res. Sect. A **275**, 133 (1989).
[20] R. A. Cecil, B. D. Anderson, and R. Madey, Nucl. Instrum. Methods **161**, 439 (1979).
[21] P. Désesquelles *et al.*, Nucl. Instrum. Methods (submitted).
[22] S. Pratt and M. B. Tsang, Phys. Rev. C **36**, 2390 (1987).